3D Ultrasonic Needle Tracking with a 1.5D Transducer Array for Guidance of Fetal Interventions

Wenfeng Xia[1], Simeon J. West[2], Jean-Martial Mari[3], Sebastien Ourselin[4], Anna L. David[5], and Adrien E. Desjardins[1]

[1] Department of Medical Physics and Biomedical Engineering, University College London, Gower Street, London WC1E 6BT, United Kingdom.
[2] Department of Anaesthesia, University College Hospital, Main Theatres, Maple Bridge Link Corridor, Podium 3, 235 Euston Road, London NW1 2BU, United Kingdom.
[3] GePaSud, University of French Polynesia, Faa'a 98702, French Polynesia.
[4] Translational Imaging Group, Centre for Medical Image Computing, Department of Medical Physics and Biomedical Engineering, University College London, Wolfson House, London WC1E 6BT, United Kingdom.
[5] Institute for Women's Health, University College London, 86-96 Chenies Mews, London WC1E 6HX, United Kingdom.
wenfeng.xia@ucl.ac.uk

Abstract. Ultrasound image guidance is widely used in minimally invasive procedures, including fetal surgery. In this context, maintaining visibility of medical devices is a significant challenge. Needles and catheters can readily deviate from the ultrasound imaging plane as they are inserted. When the medical device tips are not visible, they can damage critical structures, with potentially profound consequences including loss of pregnancy. In this study, we performed 3D ultrasonic tracking of a needle using a novel probe with a 1.5D array of transducer elements that was driven by a commercial ultrasound system. A fiber-optic hydrophone integrated into the needle received transmissions from the probe, and data from this sensor was processed to estimate the position of the hydrophone tip in the coordinate space of the probe. Golay coding was used to increase the signal-to-noise (SNR). The relative tracking accuracy was better than 0.4 mm in all dimensions, as evaluated using a water phantom. To obtain a preliminary indication of the clinical potential of 3D ultrasonic needle tracking, an intravascular needle insertion was performed in an *in vivo* pregnant sheep model. The SNR values ranged from 12 to 16 at depths of 20 to 31 mm and at an insertion angle of 49° relative to the probe surface normal. The results of this study demonstrate that 3D ultrasonic needle tracking with a fiber-optic hydrophone sensor and a 1.5D array is feasible in clinically realistic environments.

1 Introduction

Ultrasound (US) image guidance is of crucial importance during percutaneous interventions in many clinical fields including fetal medicine, regional anesthe-

sia, interventional pain management, and interventional oncology. With fetal interventions, amniocentesis, chorionic villus sampling and fetal blood sampling are commonly performed under US guidance [1, 2]. Two-dimensional (2D) US imaging is typically used to visualize anatomy and to identify the location of the needle tip. The latter is often challenging, however. One reason is that the needle tip can readily deviate from the US imaging plane, particularly with needle insertions at large depths. A second reason is that the needles tend to have poor echogenicity during large-angle insertions, as the incident US beams can be reflected outside the aperture of the external US imaging probe. In the context of fetal interventions, misplacement of the needle tip can result in severe complications, including the loss of pregnancy [2].

A number of methods have been proposed to improve needle tip visibility during US guidance, including the use of echogenic surfaces, which tend to be most relevant at steep insertion angles. However, a recent study on peripheral nerve blocks found that even with echogenic needles, tip visibility was lost in approximately 50% of the procedure time [3]. Other methods for improving needle tip visibility are based on the introduction of additional sources of image contrast, including shaft vibrations [4], acoustic radiation force imaging [5], Doppler imaging [6], and photoacoustic imaging [7]. Electromagnetic (EM) tracking has many advantages, but the accuracy of EM tracking can be severely degraded by EM field disturbances such as those arising from metal in tables [8], and the sensors integrated into needles tend to be bulky and expensive. A needle tracking method that is widely used in clinical practice has remained elusive.

Ultrasonic needle tracking is an emerging method that has shown promise in terms of its accuracy and its compatibility with clinical workflow: positional information and ultrasound images can be acquired from the same probe. With this method, there is ultrasonic communication between the external US imaging probe and the needle. One implementation involves integrating a miniature US sensor into the needle that receives transmissions from the imaging probe; the location of the needle tip can be estimated from the times between transmission onset and reception, which we refer to here as the "time-of-flights". With their flexibility, small size, wide bandwidths, and low manufacturing costs, fiber-optic US sensors are ideally suited for this purpose [9–11]. Recently, ultrasonic tracking with coded excitation was performed in utero, in an in vivo ovine model [12]. A piezoelectric ring sensor has also been used [13].

In this study, we present a novel system for ultrasonic tracking that includes a 1.5D array of 128 US transducer elements to identify the needle tip position in three-dimensions (3D). Whilst ultrasonic tracking can be performed with 3D US imaging probes, including those with 2D matrix arrays [14, 15], the use of these probes in clinical practice is limited. Indeed, 3D imaging probes tend to be bulky and expensive, 2D matrix arrays are only available on a few high-end systems, and it can be challenging to interpret 3D image volumes acquired from complex tissue structures in real-time. In contrast, the 1.5D array in this study is compatible with a standard commercial US system that drives 1D US imaging

probes. We evaluated the relative tracking accuracy with a water phantom, and validated the system with an *in vivo* pregnant sheep model.

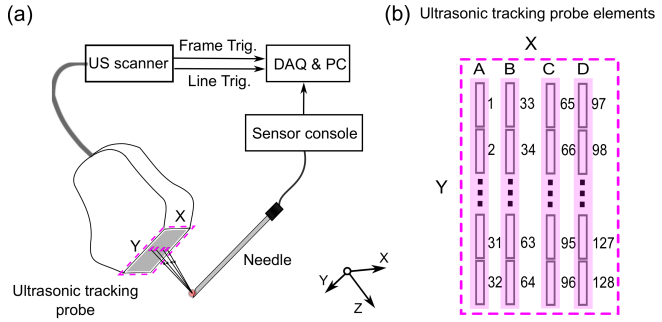

Fig. 1. The 3D ultrasonic needle tracking system, shown schematically (a). The tracking probe was driven by a commercial ultrasound (US) scanner; transmissions from the probe were received by a fiber-optic hydrophone sensor at the needle tip. The transducer elements in the probe (b) were arranged in four rows (A-D).

2 Materials and methods

2.1 System configuration

The ultrasonic tracking system was centered on a clinical US imaging system (SonixMDP, Analogic Ultrasound, Richmond, BC, Canada) that was operated in research mode (Figure 1a). A custom 1.5D tracking probe, which comprised four linear rows of 32 transducer elements with a nominal bandwidth of 4-9 MHz (Figure 1b), was produced by Vermon (Tours, France). This array was denoted as "1.5D" to reflect the much larger number of elements in one dimension than in the other. The US sensor was a fiber-optic hydrophone (FOH) that was integrated into the cannula of a 20 gauge spinal needle (Terumo, Surrey, UK). The FOH sensor (Precision Acoustics, Dorchester, UK) has a Fabry-Pérot cavity at the distal end, so that impinging ultrasound waves result in changes in optical reflectivity [16]. It was epoxied within the needle cannula so that its tip was flush with the bevel surface, and used to receive US transmissions from the tracking probe.

Three transmission sequences were used for tracking. The first comprised bipolar pulses; the second and third, 32-bit Golay code pairs [17]. Transmissions were performed from individual transducer elements, sequentially across rows (Figure 1b). The synchronization of data acquisition from the FOH sensor with US transmissions was presented in detail in Refs. [10, 11]. Briefly, two output triggers were used: a frame trigger (FT) for the start of all 128 transmissions, and a line trigger (LT) for each transmission. The FOH sensor signal was digitized at 100 MS/s (USB-5132, National Instruments, Austin, TX). Transmissions from the ultrasonic tracking probe were controlled by a custom LabView program operating on the ultrasound scanner PC, with access to low-level libraries.

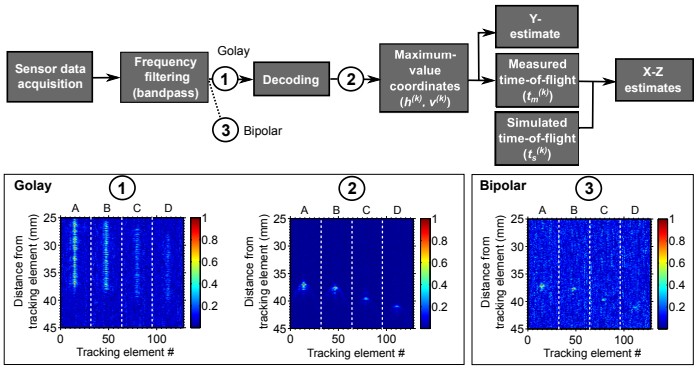

Fig. 2. The algorithm to estimate the needle tip position from the sensor data is shown schematically (top). Representative data from all transducer elements obtained before Golay decoding (1) and after (2), show improvements in SNR relative to bipolar excitation (3). These three datasets are plotted on a linear scale as the absolute value of their Hilbert transforms, normalized separately to their maximum values.

2.2 Tracking algorithms

The algorithm for converting raw FOH sensor data to a 3D needle tip position estimate is shown schematically in Figure 2. It was implemented offline using custom scripts written in Matlab. First, band-pass frequency filtering matched to the bandwidth of the transducer elements of the tracking probe was performed (Chebyshev Type I; 5th order; 2-6 MHz). For Golay-coded transmissions, the frequency-filtered data from each pair of transmissions were convolved with the time-reversed versions of the oversampled Golay codes. As the final decoding step, these convolved data from each pair were summed. The decoded data were concatenated according to the rows of transducer elements from which the transmissions originated to form 4 tracking images.

The 4 tracking images were processed to obtain an estimate of the needle tip position in the coordinate space of the tracking probe $(\tilde{x}, \tilde{y}, \tilde{z})$. The horizontal coordinate of each tracking image was the transducer element number; the vertical component, the distance from the corresponding transducer element. Typically, each tracking image comprised a single region of high signal amplitude. For the k^{th} tracking image ($k = \{1, 2, 3, 4\}$), the coordinate of the image for which the signal was a maximum, $(h^{(k)}, v^{(k)})$ was identified. The $h^{(k)}$ values were consistent across tracking images (Figure 2). Accordingly, $\tilde{y}$ was calculated as their mean, offset from center and scaled by the distance between transducer elements. To obtain $\tilde{x}$, and $\tilde{z}$, the measured time-of-flights $t_m^{(k)}$ were calculated as $v^{(k)}/c$, where c is the speed of sound. The $t_m^{(k)}$ values were compared with a set of simulated time-of-flight values $t_s^{(k)}$. The latter were pre-computed at each point (x_i, z_j) of a 2D grid in the X-Z coordinate space of the tracking probe, where i and j are indices. This grid had ranges of -20 to 20 mm in X and 0 to 80 mm in Z, with a spacing of 0.025 mm. For estimation, the squared differences between $t_m^{(k)}$ and $t_s^{(k)}$, were minimized:

$$(\tilde{x}, \tilde{z}) = \underset{(x_i, z_j)}{\arg\min} \left\{ \frac{\sum_{k=1}^{4} \left\{ [t_m^{(k)} - t_s^{(k)}(x_i, z_j)] \cdot w^{(k)} \right\}^2}{\sum_{k=1}^{4} [w^{(k)}]^2} \right\} \quad (1)$$

where the signal amplitudes at the coordinates $(h^{(k)}, v^{(k)})$ were used as weighting factors, $w^{(k)}$, so that tracking images with higher signal amplitudes contributed more prominently.

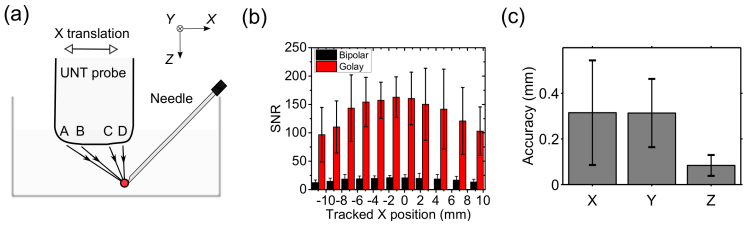

Fig. 3. (a) Relative tracking accuracy measurements were performed with the needle and the ultrasonic needle tracking (UNT) probe in water. (b) The signal-to-noise ratios (SNRs) of the tracking images were consistently higher for Golay-coded transmissions than for bipolar transmissions, and they increased with proximity to the center of the probe (X=0). The error bars in (b) represent standard deviations calculated from the four tracking images. (c) Estimated relative tracking accuracies for Golay-coded transmissions along orthogonal axes; error bars represent standard deviations calculated from all needle tip positions.

2.3 Relative tracking accuracy

The relative tracking accuracy of the system was evaluated with a water phantom. The needle was fixed on a translation stage, with its shaft oriented to simulate an out-of-plane insertion: it was positioned within an X-Z plane with its tip approximately 38 mm in depth from the tracking probe, and angled at 45° to the water surface normal (Figure 3a). The tracking probe was translated relative to the needle in the out-of-plane dimension, X. This translation was performed across 20 mm, with a step size of 2 mm. At each position, FOH sensor data were acquired for needle tip tracking.

Each needle tip position estimate was compared with a corresponding reference position. The relative tracking accuracy was defined as the absolute difference between these two quantities. The X component of the reference position was obtained from the translation stage, centered relative to the probe axis. As Y and Z were assumed to be constant during translation of the tracking probe, the Y and Z components of the reference position were taken to be the mean values of these components of the position estimates.

2.4 *In vivo* validation

To obtain a preliminary indication of the system's potential for guiding fetal interventions, 3D needle tracking was performed in a pregnant sheep model *in*

vivo [18]. The primary objective of this experiment was to measure the signal-to-noise ratios (SNRs) in a clinically realistic environment. All procedures on animals were conducted in accordance with U.K. Home Office regulations and the Guidance for the Operation of Animals (Scientifc Procedures) Act (1986). Ethics approval was provided by the joint animal studies committee of the Royal Veterinary College and the University College London, United Kingdom. Gestational age was confirmed using ultrasound. The sheep was placed under general anesthesia and monitored continuously. The needle was inserted into the uterus, towards a vascular target (Figure 4a), with the bevel facing upward. During insertion, tracking was performed continuously, so that 4 tracked positions were identified.

2.5 SNR analysis

The SNR, was calculated for each tracking image at each needle tip position. The numerator was defined as the maximum signal value attained for each tracking image; the denominator, as the standard deviation of signal values obtained from each tracking image in a region above the needle tip, where there was a visual absence of signal (20 mm $\times$ 16 tracking elements).

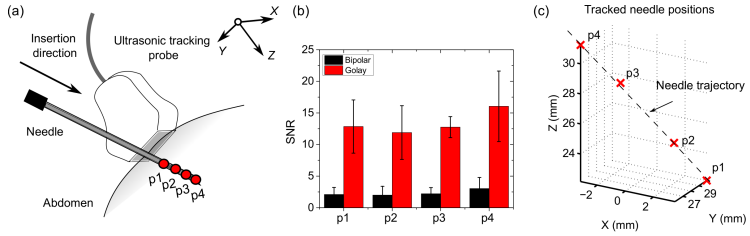

Fig. 4. *In vivo* validation of the 3D ultrasonic needle tracking system in a pregnant sheep model. (a) Schematic illustration of the measurement geometry showing the out-of-plane needle insertion into the abdomen of the sheep. The needle tip was tracked at 4 positions (p1 - p4). (b) Comparison of signal-to-noise ratios (SNRs) using Golay-coded and bipolar excitation, for all 4 tracked positions. The error bars represent standard deviations obtained at each tracked position. (c) The tracked needle tip positions, which were used to calculate the needle trajectory.

3 Results and discussion

With the needle in water (Figure 3a), transmissions from the tracking probe could clearly be identified in the received signals without averaging. With bipolar excitation, the SNR values ranged from 12 to 21, with the highest values obtained when the needle was approximately centered relative to the probe axis (X$\sim$0). With Golay-coded excitation, they increased by factors of 7.3 to 8.5 (Figure 3b). The increases were broadly consistent with those anticipated: the temporal averaging provided by a pair of 32-bit Golay codes results in an SNR improvement of $\sqrt{32 \times 2} = 8$. In water, the mean relative tracking accuracy depended on the spatial dimension: 0.32 mm, 0.31 mm, and 0.084 mm in X, Y,

and Z, respectively (Figure 3c). By comparison, these values are smaller than the inner diameter of 22 G needles that are widely used in percutaneous procedures. They are also smaller than recently reported EM tracking errors of 2±1 mm [19]. The Z component of the mean relative tracking accuracy is particularly striking; it is smaller than the ultrasound wavelength at 9 MHz. This result reflects a high level of consistency in the tracked position estimates.

With the pregnant sheep model *in vivo*, in which clinically realistic ultrasound attenuation was present, the SNR values were sufficiently high for obtaining tracking estimates. As compared with conventional bipolar excitation, the SNR was increased with Golay-coded excitation. In the former case, the SNR values were in the range of 2.1 to 3.0; coding increased this range by factors of 5.3 to 6.2 (Figure 4b). From the tracked position estimates, a needle insertion angle of 49° and a maximum needle tip depth of 31 mm were calculated.

We presented, for the first time, a 3D ultrasonic tracking system based on a 1.5D transducer array and a fiber-optic ultrasound sensor. A primary advantage of this system is its compatibility with existing US imaging scanners, which could facilitate clinical translation. There are several ways in which the tracking system developed in this study could be improved. For future iterations, imaging array elements and a corresponding cylindrical acoustic lens could be included to enable simultaneous 3D tracking and 2D US imaging. The SNR could be improved by increasing the sensitivity of the FOH sensor, which could be achieved with a Fabry-Pérot interferometer cavity that has a curved distal surface to achieve a high finesse [20]. Additional increases in the SNR could be obtained with larger code lengths that were beyond the limits of the particular ultrasound scanner used in this study. The results of this study demonstrate that 3D ultrasonic needle tracking with a 1.5 D array of transducer elements and a FOH sensor is feasible in clinically realistic environments and that it provides highly consistent results. When integrated into an ultrasound imaging probe that includes a linear array for acquiring 2D ultrasound images, this method has strong potential to reduce the risk of complications and decrease procedure times.

Acknowledgments

This work was supported by an Innovative Engineering for Health award by the Wellcome Trust (No. WT101957) and the Engineering and Physical Sciences Research Council (EPSRC) (No. NS/A000027/1), by a Starting Grant from the European Research Council (ERC-2012-StG, Proposal No. 310970 MOPHIM), and by an EPSRC First Grant (No. EP/J010952/1). A.L.D. is supported by the UCL/UCLH NIHR Comprehensive Biomedical Research Centre.

References

1. Daffos, F., et al.: Fetal blood, sampling during pregnancy with use of a needle guided by ultrasound: A study of 606 consecutive cases. Am. J. Obstet. Gynecol. 153(6), 655660 (1985)

2. Agarwal, K., et al.: Pregnancy loss after chorionic villus sampling and genetic amniocentesis in twin pregnancies: a systematic review. Ultras. Obstet. Gynecol. 40(2), 128–134 (2012)
3. Hebard, S., et al.: Echogenic technology can improve needle visibility during ultrasound-guided regional anesthesia. Reg. Anesth. Pain. Med. 36(2), 185–189 (2011)
4. Klein, S. M., et al.: Piezoelectric vibrating needle and catheter for enhancing ultrasoundguided peripheral nerve blocks. Anesth. Analg. 105, 18581860 (2007).
5. Rotemberg, V., et al.: Acoustic radiation force impulse (ARFI) imaging-based needle visualization. Ultrason. Imaging 33(1), 116 (2011).
6. Fronheiser, M. P., et al.: Vibrating interventional device detection using real-time 3-D color Doppler. IEEE Trans. Ultrason. Ferroelectr. Freq. Control 55(6), 13551362 (2008).
7. Xia, W., et al.: Performance characteristics of an interventional multispectral photoacoustic imaging system for guiding minimally invasive procedures. J. Biomed. Opt. 20(8), 086005 (2015).
8. Poulin, F.: Interference during the use of an electromagnetic tracking system under OR conditions. J. Biomech. 35, 733737 (2002).
9. Guo, X., et al.: Photoacoustic active ultrasound element for catheter tracking. Proc. SPIE 8943, 89435M (2014).
10. Xia, W., et al.: Interventional photoacoustic imaging of the human placenta with ultrasonic tracking for minimally invasive fetal surgeries. MICCAI 2015, Part I, LNCS 9349, 371378, (2015)
11. Xia, W., et al.: In-plane ultrasonic needle tracking using a fiber-optic hydrophone. Med. Phys. 42(10), 5983–5991 (2015).
12. Xia, W., et al.: Coded excitation ultrasonic needle tracking: An in vivo study. Med. Phys. 43(7), 4065–4073 (2016).
13. Nikolov, S. I.: Precision of needle tip localization using a receiver in the needle IEEE Int. Ultrason. Sym. Proc., Beijing, 479482, (2008)
14. Mung, J.: A non-disruptive technology for robust 3D tool tracking for ultrasound-guided interventions. MICCAI 2011, Part I, LNCS 6891, 153160, (2011)
15. Mung, J.: Ultrasonically marked instruments for ultrasound-guided interventions. IEEE Ultrasonics Symposium (IUS), 20532056, (2013)
16. Morris, P., et al.: A Fabry-Pérot fiber-optic ultrasonic hydrophone for the simultaneous measurement of temperature and acoustic pressure. J. Acoust. Soc. Am. 125(6), 3611-3622 (2009).
17. Budisin, S. Z., et al.: New complementary pairs of sequences. Electron. Lett. 26(13), 881–883, (1990).
18. David, A. L., et al.: Recombinant adeno-associated virus-mediated in utero gene transfer gives therapeutic transgene expression in the sheep. Human Gene Therapy 22, 419–426 (2011).
19. Boutaleb, S., et al.: Performance and suitability assessment of a real-time 3D electromagnetic needle tracking system for interstitial brachytherapy. J Contemp Brachytherapy 7(4), 280–289 (2015).
20. Zhang., E. Z.: A miniature all-optical photoacoustic imaging probe. Proc. SPIE 7899, 78991F (2011).